Epitaxial two dimensional aluminum films on silicon (111) by ultra-fast thermal deposition

Igal Levine, Alexander Yoffe, Adi Salomon, Wenjie Li, Yishay Feldman et al.

Related Articles

Epitaxial growth of Ti3SiC2 thin films with basal planes parallel or orthogonal to the surface on α-SiC
Appl. Phys. Lett. 101, 021606 (2012)

Recombination mechanisms in heteroepitaxial non-polar InGaN/GaN quantum wells
J. Appl. Phys. 112, 013534 (2012)

Growth and characterizations of semipolar (112) InN
J. Appl. Phys. 112, 013530 (2012)

Atomic behavior of carbon atoms on a Si removed 3C-SiC (111) surface during the early stage of epitaxial graphene growth
J. Appl. Phys. 111, 104324 (2012)

Suppression of threading defects formation during Sb-assisted metamorphic buffer growth in InAs/InGaAs/InP structure
Appl. Phys. Lett. 100, 152112 (2012)

Additional information on J. Appl. Phys.

Journal Homepage: http://jap.aip.org/

Journal Information: http://jap.aip.org/about/about_the_journal

Top downloads: http://jap.aip.org/features/most_downloaded

Information for Authors: http://jap.aip.org/authors

Epitaxial two dimensional aluminum films on silicon (111) by ultra-fast thermal deposition

Igal Levine,[1] Alexander Yoffe,[2] Adi Salomon,[3] Wenjie Li,[1] Yishay Feldman,[2] and Ayelet Vilan[1,a)]

[1]*Department of Materials and Interfaces, Weizmann Institute of Science, POB 26, Rehovot 76100, Israel*
[2]*Department of Chemical Research Support, Weizmann Institute of Science, POB 26, Rehovot 76100, Israel*
[3]*Department of Chemical Physics, Weizmann Institute of Science, POB 26, Rehovot 76100, Israel*

Aluminum thin films are known for their extremely rough surface, which is detrimental for applications such as molecular electronics and photonics, where protrusions cause electrical shorts or strong scattering. We achieved atomically flat Al films using a highly non-equilibrium approach. Ultra-fast thermal deposition (UFTD), at rates >10 nm/s, yields RMS roughness of 0.4 to 0.8 nm for 30–50 nm thick Al films on variety of substrates. For UFTD on Si(111) substrates, the top surface follows closely the substrate topography (etch pits), indicating a 2D, layer-by-layer growth. The Al film is a mixture of (100) and (111) grains, where the latter are commensurate with the in-plane orientation of the underlying Si (epitaxy). We show the use of these ultra-smooth Al films for highly reproducible charge-transport measurements across a monolayer of alkyl phosphonic acid as well as for plasmonics applications by directly patterning them by focused ion beam to form a long-range ordered array of holes. UFTD is a one-step process, with no need for annealing, peeling, or primer layers. It is conceptually opposite to high quality deposition methods, such as MBE or ALD, which are slow and near-equilibrium processes. For Al, though, we find that limited diffusion length (and good wetting) is critical for achieving ultra-smooth thin films. © *2012 American Institute of Physics*. [http://dx.doi.org/10.1063/1.4730411]

INTRODUCTION

Nano-technology requires controlled fabrication, at times down to the atomic level. Despite enormous progress in fabrication methods, some trivial tasks, like deposition of atomically flat metallic films still present often a serious challenge.[1] For example, in molecular electronics, ∼2 nm long molecules are commonly adsorbed onto a conducting substrate, serving as one of the electrodes. Clearly, roughness in this substrate could dominate the net transport characteristics.[2,3] Even for thicker, inorganic tunnel junctions roughness can considerably alter the tunneling behavior.[4] Plasmonics is extremely sensitive to surface inhomogeneities, which can cause scattering and reduce the propagation length of surface plasmons.[5] Consequently, inhomogeneity of the metal film surface can degrade the performance of plasmonic devices, as well as other optical applications.[6]

Aluminum (Al) is often a desired substrate, because its low work function makes it a common cathode (electron injector)[7] and its high bulk plasmon frequency of about 15 eV marks it as a promising candidate for plasmonic response in the UV region.[8] More generally Al has a wide variety of technological uses in micro-electronics and optics.[6] In the context of nanotechnology, Al is used for fabrication of ordered arrays of nano-channels using anodic oxidation.[1] Unfortunately, preparing smooth Al surfaces is especially difficult, due to the high surface mobility of Al atoms,[9] which allows them to find lowest energy positions leading to a 3D, island growth, which results in films with large surface roughness.

Deposition of Al on Si specifically was studied in the context of micro-electronics inter-connects.[10] For such purpose, island growth is detrimental because it considerably increases the electrical resistance of thin films.[11] In contrast to Al film growth for sub-monolayers coverage up to few monolayers and its in-depth characterization,[10–14] here we are interested in practical deposition of uniform, continuous films. Deposition of Al films with sub-nm roughness was reported by various methods. Rode *et al.*[15] controlled the root mean square (RMS) roughness of sputtered Al films from 100 nm to as low as 0.6 nm (on $7 \times 7 \, \mu m^2$) by varying the dc-magnetron sputtering conditions. Recently, Sun *et al.* reached a roughness <0.3 nm for thin (7 nm thick) sputtered Al films on glass, but the roughness increased sharply with film thickness (for 80 nm thick films the roughness is 1.9 nm over $1 \times 1 \, \mu m^2$).[6] However, ultra-fast sputtering at rates (17 nm/s) approaching those reported here could not get a roughness below 2 nm.[16] This study also showed that the RMS increases with the length of the scanning window up to ∼1 μm and for longer distances it saturates.[16] Atomic layer deposition (ALD) is unprecedented in its ability to preserve the underlying texture and indeed Lee and Kang[17] produced thin Al films with RMS values as low as 0.2 nm (over 1 μm^2) using ALD over 6 nm TiN on Si(100) substrates. Unfortunately, ALD is a slow and still relatively expensive process.

Film peeling or stripping is another way to obtain ultra-smooth metallic films by exposing their inner interface. In this method, a metallic film is evaporated onto a very smooth sacrificial template. The film is then glued or welded from its top

a)Author to whom correspondence should be addressed. Electronic mail: Ayelet.Vilan@weizmann.ac.il.

side to a mechanical support, and peeled from the original evaporation substrate, exposing the inner interface as the final surface.[18] Gold films with surface roughness as low as 0.2–0.4 nm over μm-wide grains[19] or even with cm-wide areas[20] can be achieved by stripping. Weiss *et al.* further extended this method to Ag (1.2 nm roughness over $5 \times 5\ \mu m^2$), Pd (0.5 nm), and Pt (0.2 nm).[21] Nagpal *et al.* used stripping to mold-pattern ultra-smooth silver films with minimal roughness of 0.34 nm (up to 1.8 nm roughness over a patterned template; measured over $5 \times 5\ \mu m^2$).[5] Smooth films by stripping were shown to considerably improve applications such as molecular electronics,[3] use in surface force apparatus[20] or plasmonics.[5,22] Peeling of very thick (50 μm) electrochemically grown Al films was used for nano-channel fabrication.[1] The major drawbacks of stripping are the additional processing steps, as well as introduction of adhesives that might be incompatible with the following processing steps.

Thermal evaporation is a standard fabrication tool. Higo *et al.* thermally evaporated Al at moderate rates (2 nm/s) and used intense annealing to reach 0.4 nm RMS surface roughness (over $1 \times 1\ \mu m^2$).[23] Annealing was reported to enhance smoothness of other metals such as gold,[24] copper,[25] and silver.[5] Nevertheless, reports on annealing of Al are sporadic and such reports were generally not reproduced in the literature. This led us to develop a more robust deposition approach to achieve highly smooth Al films, which we report on here. The key novelty is in the counter-intuitive use of extremely high evaporation rates, up to 20 nm/s. Al films, 30 nm thick, deposited on variety of smooth substrates by such ultra-fast thermal deposition (UFTD) method have record-comparable roughness levels (0.4–0.6 nm RMS/ 16 μm^2). Previous studies suggested that increased deposition rate reduces the effective incorporation of impurities, and thus, increases the grain size[26,27] and decreases the compressive stress, accounting for hillocks formation.[26]

In addition to these effects of deposition rates on the deposited films, we find that extremely high rates lead to unique film-growth behavior. On a Si(111) substrate, Al growth behaves effectively as layer by layer, preserving 1 nm steps in the underlying substrate for an up to 30 nm thick evaporated film. The Al grains showed only (111) and (100) orientations. Most surprisingly, cross-section transmission electron microscopy (TEM) reveals that the Al (111) grains were aligned with the underlying Si(111) substrate, vertically and horizontally, suggesting an epitaxial growth under kinetic-controlled deposition. We are not aware of any previous report of such film-growth mechanism. Preliminary results show UFTD to work well also for silver, indicating possible applicability for films of a range of metals, if minimal roughness is critical. We show that UFTD Al films serve as high quality substrate for both molecular electronics and for plasmonics in the UV. Finally, we give some qualitative arguments for the apparent anomalies in UFTD film growth.

MATERIALS AND METHODS

Substrates included single-side polished n-Si(111) (0.5–0.8 Ω·cm, ITME); n-Si(100) (1–10 Ω·cm, Virginia semiconductors); Quartz (SPI supplies); and optical grade quality mica sheets (S&J trading Inc.). Mica was freshly peeled prior to evaporation and all other substrates were pre-cleaned by rinsing and sonication with solvents and blown dry with N_2. Si(111) was scratched with a diamond pen on the backside, because in this way etching does not affect the very low roughness of the other surface.[28] Si wafers were etched by immersion in piranha solution (98%H_2SO_4:30%H_2O_2, 7:3, v/v; handle with care) at 90 °C for at least 30 min, rinsed with copious amounts of deionized water, and then H-terminated by deoxygenated 40% NH_4F solution for 10 min (or HF 2% for 2 min for Si(100)). Quartz pieces underwent the same treatment, excluding the final H-termination procedure. Some of the H-Si(111) substrate were plasma oxidized, using an oxygen plasma discharge (March plasmod, 13.56 MHz, 150 W, 1.5 standard cubic centimeter per minute (sccm) O_2, 1.0 sccm N_2).

Al evaporation: Al pellets, 99.999% pure (Kurt J. Lesker) were thermally evaporated (Edwards 306/2) from a Tantalum boat (6×1 cm, Mark-tech. Ltd), mounted 15 cm below the sample holder, with a manual shutter at 1 cm below the samples. XPS (Kratos AXIS ULTRA) shows no detectable Ta traces in the evaporated film (see Fig. S3 of supplementary material).[45] Replacing the Ta boat with an alumina-coated tungsten boat (Lesker) leads to similar film roughness (see Fig. S4 supplementary material).[45] The samples were near room-temperature, because they were mounted on fair heat-sink (1 cm thick brass stage) and computations show (see Tables S1 and S2 of supplementary material)[45] that evaporation heat the sample at the very most by a few degrees above room-temperature. The evaporator base pressure was 5×10^{-6} mbar and increased up to 8×10^{-6} mbar during evaporation. Residual gas analysis (RGA, Inficon transpector 100) indicates oxygen partial pressure of 3×10^{-11} (see Table S3 of supplementary material for complete composition).[45] Prior to reaching the melting point, the boat was heated 60 s for degassing, which was then followed by further heating to achieve complete melting of the Al. The evaporation rate was measured with a pre-calibrated quartz monitor. The evaporation rate increased slowly with a closed shutter (this stage might help reducing residual gases) until the rate exceeded 10 nm/s, when the shutter was opened for 1–3 s. Al was then evaporated at an average rate of ~20 nm/s to a total thickness of ca. 30–50 nm, as measured with a Dektak profilometer and verified using cross section TEM.

Atomic force microscopy (AFM) was done using an ambient AFM P47 (NT-MDT, Zelenograd, Russia), with a small range scanner in the tapping mode over an area of 16 μm^2. The cantilever type was "Olympus 240" (nominal resonant frequency: 70Khz). X-ray diffraction (XRD) was performed on a MAX/B Rigaku diffractometer with an IU 200 x-ray generator from Rigaku. High-resolution scanning electron microscopy (SEM) was done using a Supra-55 VP Zeiss apparatus. Cross-section TEM was done with a Philips Tecnai F20 Super Twin on Si(111)/Al (30 nm)/AlOx/ $PO_3(CH_2)_{12}CH_3$/Cr (2 nm)/Au (20 nm) samples which were cross-sectioned into 100 nm wide lamellas in a dual beam FEI Helios 400 s focused ion beam (FIB) system with standard lift-out method, followed by 5 kV and then 2 kV final thinning steps for removing possible Ga ion implantation and dust re-deposition during the milling process. Nano-

pattering of the Al films was done by using the same FIB with an ion beam current of ~50 pA.

Alkyl phosphonic acid (APA) monolayers were adsorbed on these Al substrates by overnight immersion in a 5 mM iso-propanol solution of dodecane phosphonic acid as detailed elsewhere.[29] Current-voltage curves were recorded in a N_2 environment (10% relative humidity), using 99.9999% pure (~0.5 mm diameter) Hg droplets (controlled growth mercury electrode, Polish Acad. of Sciences) in a voltage scan mode (steps of 0.01 V), using a Keithley model 6430 sub-fA remote source meter.

RESULTS

Most of our work used H-terminated Si because this is a very smooth (~0.4 nm) substrate, also macroscopically and it is electrically conductive. H-Si was preferred over Si with a native oxide to be sensitive to substrate crystal structure and to minimize residual water. Nevertheless, we later found that the details of the substrate are of minor importance for the roughness of UFTD films.

UFTD of Al films, at rates >10 nm/s, yielded films with roughness between 0.4 and 0.6 nm, as can be seen in Fig. 1 from 4 × 4 μm AFM images of UFTD Al films on Si(111) and Si(100) substrates. The RMS of the surface roughness was derived from similar 4 × 4 μm AFM images recorded after each evaporation. A fast evaporation rate was found to be critical for minimizing the roughness as shown in Fig. 2. Slower deposition rates (0.01–0.1 nm/s) yielded rougher Al films (RMS>1.5 nm). The power law dependence of roughness on deposition time implies that a two-fold reduction in roughness requires a four-fold faster deposition. While this might seem feasible, such deposition rates are actually technically challenging. The power law observed in Fig. 2 is also
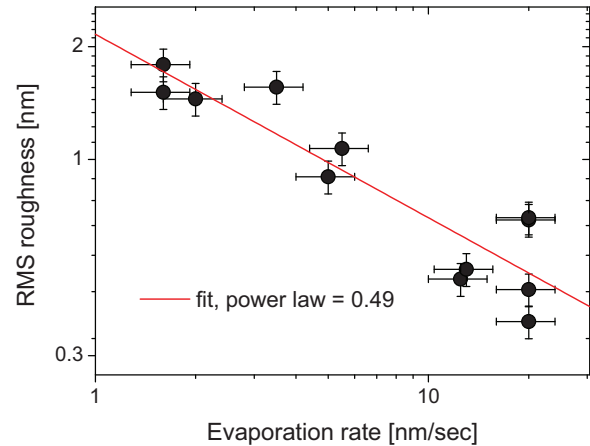
FIG. 2. RMS surface roughness measured by AFM as a function of the deposition rate of Al on H-Si(111) surfaces. The line is a fit to a power law (see Eq. (2)).

supported by fitting the data of Rode *et al.*,[15] on sputtering of Al (Fig. S2(a) of supplementary material).[45]

Slow deposition rates (≤0.1 nm/s) also caused extended film oxidation,[27] as seen by a brownish-silvery color of the evaporated film. Realizing this critical role of minute amounts of O_2 in the chamber,[15,27,30,31] it was important to assure that the pressure inside the chamber was below 10^{-5} mbar. Medium evaporation rates (1–5 nm/s) yielded silvery-bright surfaces, but with relatively poor roughness (RMS ~ 1.0–2.0 nm). High evaporation rates, exceeding 10 nm/s, yielded films with roughness between 0.4–0.6 nm. Low surface roughness was limited to thin films. Films of 30 to 50 nm thick were routinely evaporated with excellent smoothness, however, a few attempts to increase film thickness to 200 nm yielded surface
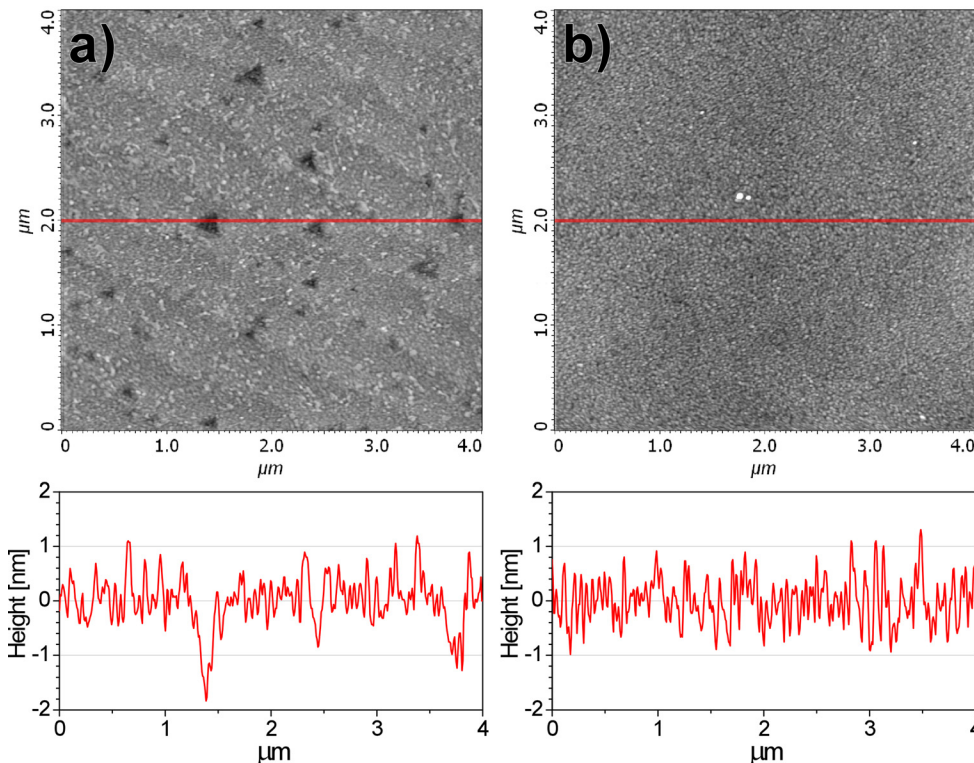
FIG. 1. Typical AFM images of Al deposited on (a) Si(111) and (b) Si(100). The RMS surface roughness of both (a) and (b) is ~0.4 nm. Each plot is 4 × 4 μm and the gray scale corresponds to 0 to 4 nm height. Bottom panels are section analyses along the horizontal red line (of top panels), showing that the typical peak-to-valley values are <2 nm.
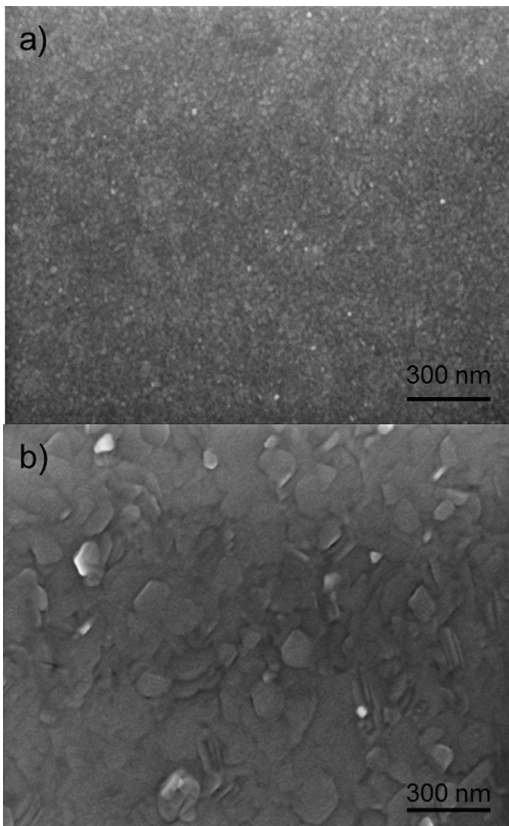
FIG. 3. SEM images of Al deposited on Si(111). (a) Thin Al film (∼45 nm) with RMS surface roughness of 0.6 nm. (b) Thick Al film (∼200 nm) with RMS surface roughness of 2.0 nm. Both films were deposited in high rates (∼20 nm/s).

roughness of ∼2.0 nm RMS. Fig. 3(b) shows large randomly oriented platelets for a 200 nm thick UFTD Al film, platelets which are completely absent in the 30 nm film (Fig. 3(a)).

One of the fascinating features in Fig. 1 is that we see triangles and diagonal steps for the Al film deposited on H-Si(111) (Fig. 1(a)). These features are typical for the underlying H-Si(111) substrate (etch pits), and are not observed for H-Si(100) (Fig. 1(b)). The height of the triangular features on the H-Si(111) surface is about ∼1 nm, and Fig. 1(a) reveals them at the surface of a 30 nm thick Al film. The comparison of two different Si orientations indicates that the crystal plane of the underlying substrate does not affect the roughness (see also Table I).

TABLE I. Surface roughness before and after Al and Ag UFTD onto different substrates.

	Substrate		UFTD	
Substrate	RMS[a]	Metal	RMS[a]	Peak to peak[b]
H-Si(111)	0.2–0.3	Ag	1.20	4.0–8.0
H-Si(111)	0.2–0.3	Al	0.4–0.6	1.0–2.0
SiOx/Si(111)	0.2–0.3	Al	0.4–0.6	1.0–2.0
H-Si(100)	0.2–0.3	Al	0.4–0.6	1.0–2.0
Mica	<0.1	Al	0.8	2.0–3.5
Quartz	1.0	Al	0.8	2.0–4.0

[a]RMS roughness in nm was computed over 16 μm^2 area.
[b]Peak to peak, in nm equals the difference between maximum and minimum height over the 16 μm^2 area.

TEM of a cross section provides further confirmation of the high quality of UFTD Al films, as shown in Fig. 4. In contrast to the exaggerated height/width ratio of AFM images, TEM (Fig. 4(a)) shows extremely mild surface undulations along 300 nm. Combining AFM and TEM information suggests a wave-like nature of the surface, with 1–2 nm amplitude and a wavelength of ∼50–100 nm. The thickness of the Al film, as measured by TEM, was about 30 nm, and that of the AlOx was found to be around 3 nm.

High resolution TEM (HR-TEM) (Fig. 4(b)) shows a sharp interface between the Si(111) substrate and the UFTD Al film, which shows up as a ∼30% decrease in the lattice fringe spacing.[10] The high resolution image (Fig. 4(b)) shows the lattice fringes to abruptly change from Si to Al with no indication for an amorphous interface (e.g., interface oxidation), which is how the interfacial contrast of the low-resolution image (Fig. 4(a)) could be interpreted.

The spacing between the lattice fringes of the Al reveals that the Al crystal orientation is (111), which is aligned with the Si(111) plane, as confirmed by the selected area diffraction (SAD) pattern shown in Fig. 4(c), where the inner spots belong to the Si diffraction and the outer ones are from the Al. As shown in Fig. 4(c), the diffraction spots of the Si substrate and Al film are exactly along the same line for both ⟨111⟩ and ⟨100⟩ directions, which indicates that the Al film is aligned with the Si substrate not only in the growth direction (vertically) but also in-plane (horizontally). This provides clear evidence that the underlying Si induced the orientation of the top UFTD Al film. Alignment occurs despite the large (30%) mismatch between the Al(111) and Si(111) spacing because 3 translations of Si(111) match 4 translations of Al(111).[10]

Not all the Al grains had the (111) orientation and some had the (100) orientation that yields no diffraction (SAD) signal. Cross section bright field TEM was used to measure the grain sizes, and the orientation of each grain was deduced from the presence or absence of SAD. Grain analysis reveals that the average grain size of the Al(111) crystals is 240 ± 170 nm and that of the Al(100) crystals is 110 ± 65 nm, corresponding to 8 or 4 times the thickness of the film (30 nm). The width of these flat grains is similar to the apparent size of the 3D grains in very thick films (Fig. 3(b)). These are very large grain sizes compared to sputtered Al films, for which a grain size of 230 nm was reached only for film thickness of 200 nm,[16] though smaller than in MBE-Al films, where grain size is ∼15 times the film thickness.[11] Furthermore, large grain size is commonly accompanied with high roughness (∼2–3 nm for sputtering[32] and tens of nm for MBE[11]), in contrast to our observation.

Orientation of the Al crystallites *over a large area* is better characterized by XRD, as shown in Fig. 5. XRD shows UFTD Al film to be poly-crystalline, with only (111) (at 2Θ = 38.47°) and (100) orientations (only the (200) diffraction is allowed, and seen at 2Θ = 44.74°). The ratio between the two groups of Al crystallites varied across the 5 samples that were measured, from 20:1 to 1:4 ((111):(200)). For evaporated Al, (111) is known to be the stable orientation, because this plane has the lowest surface energy.[26,33] Sputtered Al films were reported to evolve from 50% (111) orientation for thin films (100 nm thick) to 93% (111) orientation
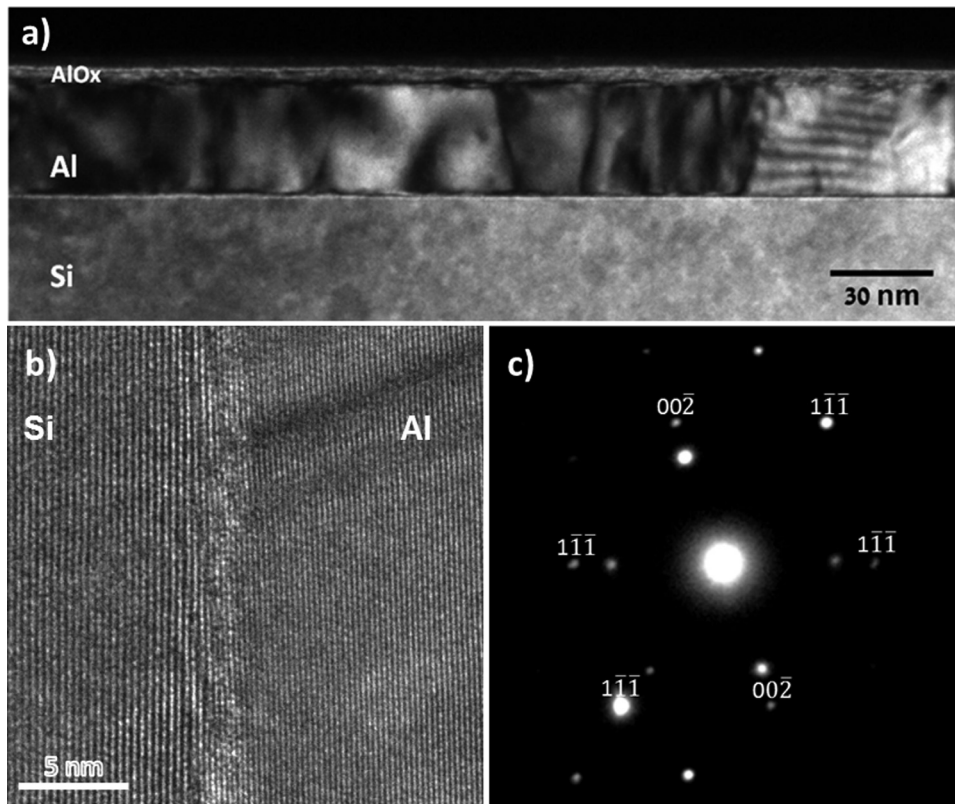
FIG. 4. Cross-section TEM image of Al film deposited on Si(111). (a) Wide view; (b) high magnification (scale bar is approximated); (c) selected area diffraction pattern with indicated directions. The thickness of the Al film is 30 nm, and that of the amorphous AlOx is 3 nm.

for thick films (1 μm),[16] while MBE Al films showed (111) orientation, regardless of thickness.[11] One of our UFTD Al samples on Si(100) was even amorphous (gave no Al peaks in XRD), which is an indication for the non-equilibrium nature of UFTD as further considered in Section "Discussion."

To examine if the surface chemistry affects the film-growth mechanism,[13,14] we compared different pre-treatments of the Si(111) substrates prior to evaporation. In addition to the above-reported hydrophobic H-terminated Si, we also tested a hydrophilic oxidized Si(111) surface, prepared by O_2 plasma oxidation of the H-Si (prepared as before). Oxidation turns the surface from hydrophobic to hydrophilic, introduces hydroxyl groups on the surface and is expected to increase the Al wetting of the surface. In addition, other smooth substrates
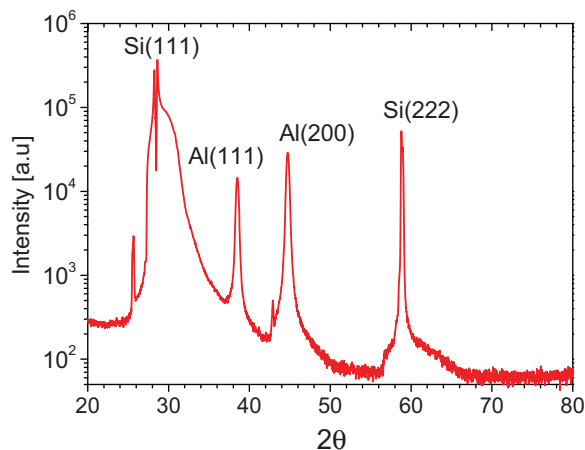
such as mica and quartz were tested in an attempt to identify key features controlling the film-growth mode. The AFM-measured surface roughness for all these films is summarized in Table I.

Table I indicates that the roughness values were slightly higher for oxidized surfaces (quartz and mica) than for Si, of both orientations. One would expect that the smoother the target substrate is, the smoother will be the obtained deposited film.[23] Clearly this is not the case with UFTD, as the mica used for the deposition had a surface roughness of 0.1 nm or less, lower than the crystalline Si (RMS $\sim$ 0.2–0.3 nm). In contrast, the deposited film under the same deposition conditions was 1.5–2 times rougher on mica than on the Si (although still quite smooth). Weak interactions with the substrate favor island growth (Volmer-Weber mode) and mica is known to promote such growth mode.[34] Thus, despite its smoothness, the poor wettability of mica undermines its performance as a substrate for achieving ultra-smooth films.

Quartz is interesting because even if the top Al roughness is not as good as that over Si, it is lower than the roughness of the underlying quartz substrate, as if the UFTD film filled-in the grooves of the original surface. A similar smoothing effect was reported for sputtering of Al on Ti.[35] Thus, quartz does not induce a layer by layer growth as does Si(111), probably due to its amorphous surface (see Discussion).

In principle, the oxidized surfaces could also increase the amount of co-deposited water.[31] However, no difference in roughness was observed between oxidized and H-Si. This finding, which is also relevant for deposition on mica and quartz, suggests that substrate surface hydrophilicity does not play an important role under UFTD conditions. Overall, Table I shows that despite the observed slight sensitivity to

FIG. 5. Representative x-ray diffraction pattern of UFTD Al film on Si(111). Diffraction peaks are labeled in the plot.

specific surface details, UFTD is rather indifferent to the substrate and leads to excellent smoothness over a wide range of non-metallic substrates.

Finally, we suggest that the UFTD is not limited to Al films, as can be seen from the Ag example of Table I. While the Ag smoothness is poorer than that of Al, it is as good as that reported for stripped Ag[21] (though poorer than that reported in Ref. 5). We note, though, that in our work on Ag deposition details were not optimized (as was done for Al) so that Ag smoothness might be further improved.

APPLICATIONS

Molecular electronics studies charge transport across organic molecules. As the molecules are normally 1–2 nm long making electronic junctions that include the molecules therefore requires high fabrication precision. One of the popular configurations for preparing such molecular junctions is by adsorbing a molecular monolayer on a substrate that serves also as contact to the molecules, where the second contact is deposited on the free surface of the molecules by various techniques.[36] Naturally, substrate roughness in the order of the molecular length (1–2 nm) easily leads to the transport being dominated by defects, rather than by the studied molecules. This is expressed by a large span of the current-voltage (*J-V*) curves, as found in the case of alkyl-thiols on Ag.[3]

The smooth Al films, deposited on Si(111), were tested as substrate for the molecules, and thus, as one of the electrodes in a metal-molecule-metal (MMM) junction, comprised of alkyl chains, containing 12 carbons (C12), bound via a phosphonate link (total length 1.7 nm) to the Al oxide, and liquid Hg as top electrode (see inset of Fig. 6). The measured *J-V* curves across these junctions are shown in Fig. 6. The maximum variation between the 16 *J-V* curves recorded over 3 different substrates (with no data filtering) was as a factor of 5. This is significantly better than the ∼100 fold variation reported for C12 thiol on stripped Ag,[3] a result that already was a great improvement over the 5 orders of magnitude var-

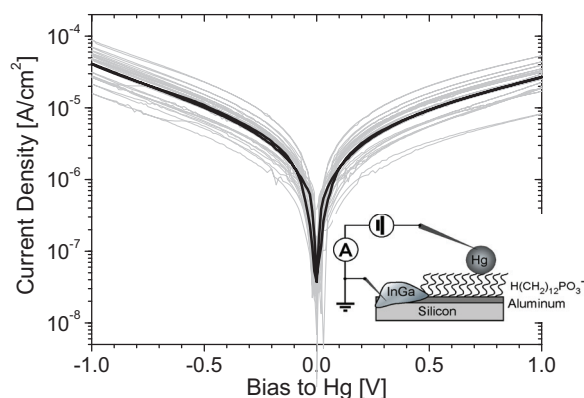FIG. 6. Current-voltage (*J-V*) curves measured across a self-assembled monolayer of C12 alkyl phosphonate on UFTD Al film on Si(111) with RMS roughness of 0.6 nm. Each gray curve was on a different junction and black line is logarithmic average. The total spread in current (max/min) is about a factor of 5. The inset shows schematically the measurement setup (not to scale). The current flow from the top Hg contact across the monolayer to the Al substrate and collected by the InGa "back" contact.

iation in current with the as-deposited Ag film (5 nm RMS roughness).[3] The excellent reproducibility in *J-V* measurements suggests that the Al/monolayer/Hg junction is a reliable and robust test-bed for large-area molecular electronics. We have reported elsewhere a detailed study over various monolayer chain lengths on Al films.[29]

We further explore the possibility to use ultra-smooth Al films for nano plasmonic application. Commonly used metals for nano-plasmonic applications, such as Au and Ag, are limited in the UV region because their bulk plasmon frequency, ω_p, is about 2.4 eV and 3.6 eV, respectively. As mentioned above, the intrinsic properties of Al make it the best metal for surface plasmon excitation in the UV region. Yet, fabrication of regular nm-sized holes is difficult due to high surface roughness and relatively large Al grains, something that can degrade the performance of the plasmonic device. By using FIB, we could directly drill nm-sized holes inside the smooth Al films. Fig. 7 shows examples of state-of-the-art direct patterning in Al films, evaporated both on quartz and silicon. Both long range patterns and high resolution single holes can be easily fabricated without additional means. Furthermore, the film roughness after patterning was less than 0.5 nm. This is important, as such low roughness should reduce scattering processes, and is expected to yield a high performance of the plasmonic device.

DISCUSSION

The UFTD behavior that we observe is rather puzzling. How can such rapid, rough deposition provide film quality close to what can be obtained by MBE or ALD? What drives the low roughness as well as the layer by layer growth? Among the critical parameters which are known to affect thin-film morphology,[31,37] the deposition rate is often overlooked. When it is considered then deposition rate is mostly related to indirect effects, such as decreasing the compressive stress[26,38] or reducing the impingement ratio of impurities.[26,27] In principle, the rapid deposition increases the super-saturation[26] and restricts the diffusion distance. At this stage, we cannot give a detailed mechanism, but we venture to suggest a qualitative explanation.

The observed trend (Fig. 3) of a smooth, continuous thin film that breaks into platelets at higher thickness is also opposite to commonly observed cluster growth that turns into a continuous film.[32,39] The structure-zone model predicts the texture of a thin film according to the ratio of substrate temperature to the melting temperature. For Al, deposited near room temperature this ratio is 0.32, corresponding to "T-zone" growth mode, of fast surface diffusion but restricted grain-boundaries diffusion.[31] A "T-zone" film growth is characterized by small, randomly oriented grains near the substrate that coalesce into larger grains with increasing thickness.[31] Similar to the "T-zone" model, Fig. 3 suggests that the crystals change their equilibrium shape, however, their size hardly changes, but rather the grains change from 2D to 3D ones for thin and thick films, respectively.

Sloope and Tiller have noted that $log(F)$ (*F* for deposition rate) and reciprocal temperature are the two basic parameters that map the transitions from amorphous to
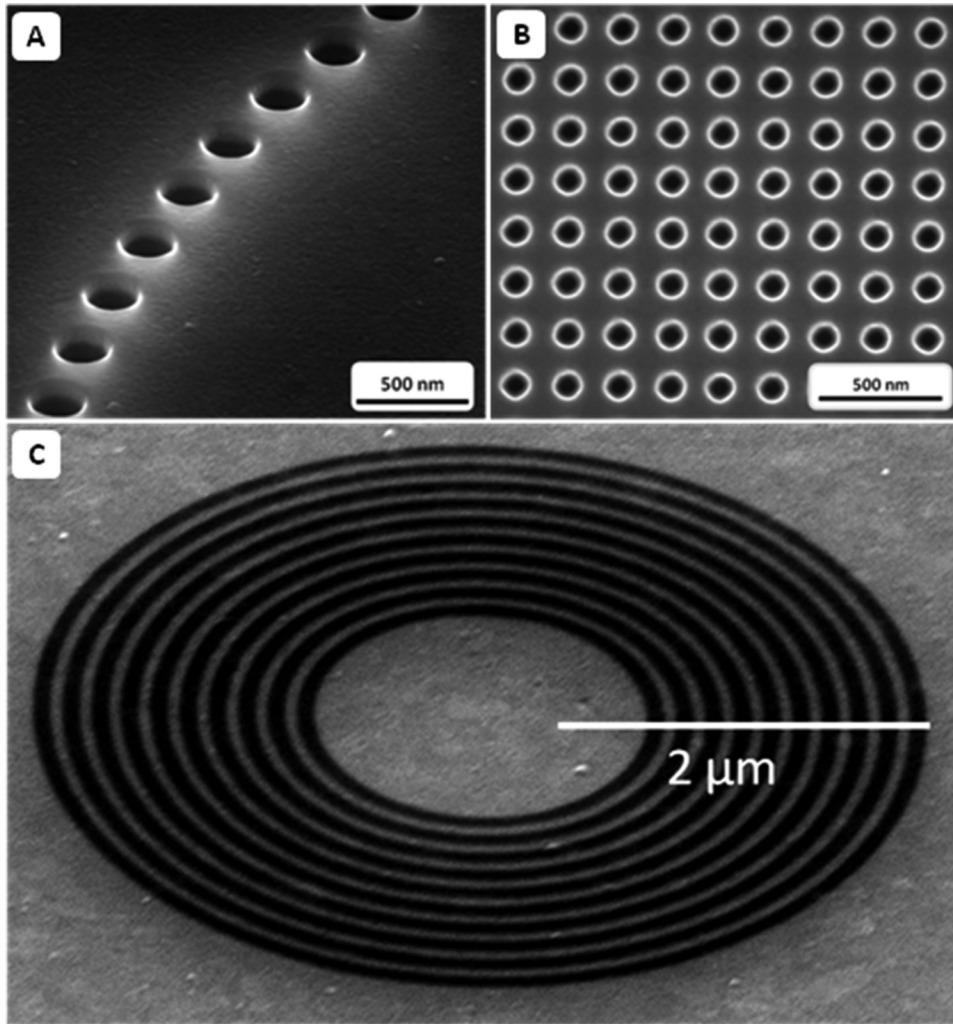
FIG. 7. SEM images of FIB fabricated nano structures by directly milling a 50 nm thick Al film made by UFTD on quartz. (a) Holes of $\sim$200 nm diameter, taken at 52 tilt. (B) A 50 μm hole array of $\sim$100 nm diameter. (c) "bull's eye" structure with about 1.5 μm circular grooves of $\sim$40 nm depth, with periodicity of about 150 nm, taken at 52° tilt.

poly-crystalline and even mono-crystal growth.[40] Their basic consideration was the nucleation rate, which is proportional to F^n, where $n \geq 2$ is the number of atoms in the smallest stable cluster.[40] We can extend this view and suggest that the roughness depends reciprocally on the nucleation rate, but the difference between observed power law (0.5) and nucleation prediction (≥ 2) does not support this view, unless nucleation rate has an indirect effect.

Another possible rate-related argument is the counter-intuitive role that diffusion plays in UFTD. Diffusion is intuitively taken to ease stresses, and if roughness is considered as noise than it should decrease with higher diffusion.[5,12,20,23] However, for systems which tend toward 3D island growth (Volmer-Weber growth)[34,37] roughness is not noise but an equilibrium state, and for such systems diffusion would increase roughens. Indeed, most metals tend to 3D island growth on substrates of low surface energy such as mica, quartz or Si.[34] The high surface diffusion of Al[9] allows the arriving atoms to move over a long distance on the surface to find their lowest energy positions, namely to build-up only a few, but large 3D crystals, as can be seen in Fig. 3(b).

Our qualitative suggestion is inspired by a description of roughness that uses scaling concepts.[41] Normally, the scaling is done with respect to the amount of deposited material, or time of deposition (for a constant deposition rate).[32,41] Such time evolution is practically impossible with the extremely rapid rates we used here. However, a natural scaling parameter for these stochastic models is the *diffusion length*, L_D, i.e., the length that an adatom diffuses before another adatom arrives[42]

$$L_D = \sqrt{D/F}, \tag{1}$$

where D is the lateral diffusion constant (in area per time) and F is the deposition rate (in atoms per time). Amar *et al.* used L_D as a scaling factor for predicting island density and the fractal dimension below 1 ML coverage.[42] We use this concept to describe roughness of a multi-layer film. While for the detailed growth mechanism we may need to add different scaling powers, still we can crudely estimate that the roughness is linearly proportional to the diffusion length, L_D, and therefore, to the deposition rate, F

$$RMS \propto L_D \propto F^{-0.5}. \tag{2}$$

Considering that diffusion is temperature activated,[9] Eqs. (1) and (2) also predict that the roughness will increase with temperature according to

$$RMS \propto exp\left(\frac{-E_D}{2k_BT}\right), \qquad (3)$$

where E_D is the diffusion energy and the factor of 2 is because of the square root in Eq. (1). The power law fit to the experimental data of Fig. 2 gave a slope of -0.49, in excellent agreement with Eq. (2). No correlation was observed with film thickness (Fig. S1(a) of supplementary material)[45] and a power law relation correlated the data better than logarithmic decay or a linear relation (Fig. S1(b) of supplementary material).[45]

Strong support for the applicability of the diffusion length concept comes from the good correlation of Eqs. (2) and (3) to literature data, reported by Rode *et al.* on the roughness of *sputtered* Al films (Fig. S2 of supplementary material, Ref. 45).[15] The clear smoothing effect that cooling has on the sputtered Al films (Refs. 15 and 26; Fig. S2(b) of supplementary material)[45] suggests that cooling could improve smoothness also for evaporated films. We note, though, that cooling was suggested to increase the compression stress in the film and leads to hillocks formation.[26] We did not observe such hillocks, but possibly cooling to lower temperatures might lead to that.

A major weakness of the diffusion argument is that a rough estimate of L_D yields numbers less than the interatomic distance. In principle, increasing the deposition rate could also have indirect effects, such as less sample heating. We dismiss this option because calculations show that even at the slowest deposition rate the heating does not exceed a few degrees (see Table S2 of supplementary material).[45] Another indirect effect would be the incorporation of impurities, such as oxygen. Barna *et al.* showed that the grain size of evaporated Al varies as a power law of -0.5 with the oxygen to aluminum impingement ratio.[27] In principle, this ratio is inversely proportional to the deposition rate, but the relation between grain size and roughness is not straightforward. If larger grains imply higher roughness than the trend of Fig. 2 is opposite to the one, induced by oxygen.[27] In addition, the O_2/Al impingement ratio here ($\leq 2.4 \times 10^{-4}$) is well below the lowest ratio (0.01) reported.[27] A clear effect of residual oxygen on Al morphology and orientation was also reported by Verkerk and van der Kolk for partial O_2 pressure above 10^{-9} Torr,[43] above the partial O_2 pressure in our case (3×10^{-11}).

Another explanation relies on thermodynamics. A higher evaporation rate, F drives the equilibrium from 3D (rough) toward 2D (flat) by increasing the super-saturation (F/F_{eq}) of the evaporated atoms, and thus, their chemical potential ($\Delta\mu = k_BT\ln\left(\frac{F}{F_{eq}}\right)$), where subscript *eq* indicates equilibrium).[34] This is because super-saturation reduces the "line tension" and therefore the critical island size (the minimal nucleus size which is stable).[12] Li and Hu also included the ratio between diffusion and deposition rate as a parameter in their computations of chemical energy in addition to the elastic energy as a driving force toward 2D growth.[39] The nucleation density also increases with the deposition rate[12,40] and very dense nucleation leads to fast coalescence of grains, an effect that is required to explain the very wide grains observed by HR-TEM (i.e., the final number of grains

is much smaller than the nucleation density under UFTD conditions).

Still, the UFTD film is apparently a meta-stable phase as evident from the coexistence of the metastable (100) orientation and energetically favored (111) orientation,[9,10,17] and even the amorphous Al that is occasionally observed on Si(100). We speculate that the poor reproducibility of the ratio of (111) to (100) crystallites expresses minor changes in evaporation rate or sample temperature between different preparations. In addition, Fig. 3 shows that the meta-stable smooth Al films evolve with time into 3D platelets. Annealing of a UFTD Al film at 300 °C for 3 h under Ar atmosphere led to slightly larger grains of hillock-like structures and an overall higher RMS surface roughness. In contrast, the FIB beam induces milder annealing, possibly by introducing localized defects, and the surface of the FIB-treated Al films seemed actually smoother than before the FIB work on it. All the points given above indicate that rough 3D morphology is the energetically favored phase, in accordance with a threshold thickness of ~30 nm, which was identified as that which separates independent 3D island growth from a continuum, 2D growth, for sputter-deposited Al films.[6,32]

The observed epitaxy is highly unusual for the super-saturation conditions used here.[12] We suggest that the UFTD grains do not grow by isolated sticking of adatoms, but rather by coalescence of an amorphous layer or many tiny nuclei into a long ordered (up to ~200 nm) crystallite. Small nuclei have a low rotation barrier to re-orient along the energetically favored epitaxial direction.[12,34] Such scenario also explains the much larger lateral size of the grains (~200 nm) compared to their height (~30 nm), in contrast to previous reports.[6,32] There was a considerable difference between the roughness periodicity as observed from the top by AFM (Fig. 1) and by SEM (Fig. 3) and that deduced from high resolution TEM on cross-sections of the films. This is probably because the top roughness is due to top-grain ridges and not real grain-boundaries.[16]

The layer by layer growth of Al on Si(111), as evident from the accurate replication of the 1 nm deep Si etch pits on the top surface of a 30 nm thick film (Fig. 1(a)), seemingly requires an efficient interlayer (vertical) matter flow,[12] which apparently contradicts our claim of super-saturation and negligible diffusion time in UFTD. Structural defects, such as step edges could exert, in certain cases, a long-range attraction force that funnels adatoms to fill the defects. One origin of such attraction to step-edges could be elimination of high energy surface states induced by step-edges, as was found by density functional theory (DFT) for Al deposition on Al.[9] STM studies on the growth of Pb on Si(111) showed a layer by layer growth that is controlled by the quantum size effect, namely preferred island heights, due to deeper electronic energy levels.[44] Both effects are driven by electronic energies and known to work at low temperatures,[9,44] because they originate in active attraction and not in diffusion. It is reasonable that the nature of this attraction force is substrate-dependent, and therefore, layer by layer growth was observed on Si(111) (preserved substrate features) and not on quartz (where substrate roughness was smoothened).

Although the above electronic smoothing effect might be specific to certain metals or substrates, the ability of

UFTD to get low-roughness films is fairly general. Specific surface interactions possibly alter diffusion/sticking. The rougher Al on mica might be due to the very poor wetting of mica compared to other substrates. Nevertheless, the high deposition rate does not enable too much surface diffusion and build-up of large crystals on any of the tested surfaces. Rode *et al.* identified the reduced relative amount of O_2 as the main cause for the improved smoothness.[15] Our high resolution TEM (Fig. 4(b)) shows an abrupt Si-Al interface without an amorphous oxide, although the slight change in contrast could be attributed to dis-continuous oxide patches at the Si-Al interface. Still the use of an oxidized Si substrate (Table I), with possibly more residual water than on H-Si, did not increase the roughness. Thus, while we cannot ignore the possibility of some interface oxidation, we suggest that the kinetic argument is an important factor, universal to a large class of metallic thin films deposited by either evaporation or sputtering, on various non-wetting substrates.

CONCLUSIONS

Smooth Al films can be "ready-made" at room temperature, by thermal evaporation at very high speeds, on a variety of substrates. The fast evaporation concept of UFTD probably can be extended to various metals beyond Al, and it is specifically appropriate for metals of high surface diffusion on non-wetting substrates that tend to 3D island growth. The non-equilibrium, kinetically controlled UFTD leads to epitaxial, layer by layer growth of Al on Si(111) for film thickness up to 50 nm. Restricting the diffusion length, $\sqrt{D/F}$, is a simple rule of the thumb that fits nicely to both our data as well as to those on sputtered Al films, reported by Rode *et al.*[15] It offers practical means to decrease the roughness by extremely high deposition rates and/or by cooling the substrate. Achieving such ultra-flat films of Al specifically, and of other metals in general fills a critical need for various nanotechnology related endeavors, such as molecular (bio)electronics, plasmonics, and sensors, where surface roughness poses a major obstacle in utilizing nano-scale phenomena.

[1]S. Biring, K.-T. Tsai, U. K. Sur, and Y.-L. Wang, Nanotechnology **19**, 015304 (2008).

[2]Y. Jin, N. Friedman, M. Sheves, and D. Cahen, Langmuir **24**, 5622–5626 (2008).

[3]E. A. Weiss, R. C. Chiechi, G. K. Kaufman, J. K. Kriebel, Z. Li, M. Duati, M. A. Rampi, and G. M. Whitesides, J. Am. Chem. Soc. **129**, 4336 (2007).

[4]C. W. Miller, Z.-P. Li, J. Akerman, and I. K. Schuller, Appl. Phys. Lett. **90**, 043513 (2007).

[5]P. Nagpal, N. C. Lindquist, S.-H. Oh, and D. J. Norris, Science **325**, 594–597 (2009).

[6]Z. Sun, C. Cao, L. Cao, P. Liang, X. Huang, and X. Song, Vacuum **84**, 828 (2010).

[7]Y. Vaynzof, T. J. Dennes, J. Schwartz, and A. Kahn, Appl. Phys. Lett. **93**, 103305 (2008).

[8]E. D. Palik, *Handbook of Optical Constants of Solids* (Academic, London, 1985).

[9]R. Stumpf and M. Scheffler, Phys. Rev. B **53**, 4958–4973 (1996).

[10]R. M. Groger and M. R. Barczewski, Surf. Interface Anal. **32**, 154–160 (2001).

[11]N. Joshi, A. K. Debnath, D. K. Aswal, K. P. Muthe, M. S. Kumar, S. K. Gupta, and J. V. Yakhmi, Vacuum **79**, 178–185 (2005).

[12]Z. Zhang and M. G. Lagally, Science **276**, 377 (1997).

[13]T.-C. Shen, C. Wang, and J. R. Tucker, Phys. Rev. Lett. **78**, 1271–1274 (1997).

[14]D. P. Adams, T. M. Mayer, and B. S. Swartzentruber, J. Appl. Phys. **83**, 4690–4694 (1998).

[15]D. L. Rode, V. R. Gaddam, and J. H. Yi, J. Appl. Phys. **102**, 024303 (2007).

[16]A. E. Lita and J. E. Sanchez, Jr., J. Appl. Phys. **85**, 876–882 (1999).

[17]Y. J. Lee and S.-W. Kang, J. Vac. Sci. Technol. A **20**, 1983–1988 (2002).

[18]M. Hegner, P. Wagner, and G. Semenza, Surf. Sci. **291**, 39 (1993).

[19]B. Atmaja, J. Frommer, and J. C. Scott, Langmuir **22**, 4734 (2006).

[20]L. Chai and J. Klein, Langmuir **23**, 7777 (2007).

[21]E. A. Weiss, G. K. Kaufman, J. K. Kriebel, Z. Li, R. Schalek, and G. M. Whitesides, Langmuir **23**, 9686 (2007).

[22]N. C. Lindquist, P. Nagpal, A. Lesuffleur, D. J. Norris, and S.-H. Oh, Nano Lett. **10**, 1369 (2010).

[23]M. Higo, K. Fujita, M. Mitsushio, T. Yoshidome, and T. Kakoi, Thin Solid Films **516**, 17–24 (2007).

[24]Y. Golan, L. Margulis, and I. Rubinstein, Surf. Sci. **264**, 312–326 (1992).

[25]I. Platzman, C. Saguy, R. Brener, R. Tannenbaum, and H. Haick, Langmuir **26**, 191 (2009).

[26]C. Y. Chang and R. W. Vook, J. Vac. Sci. Technol. A **9**, 559–562 (1991).

[27]P. B. Barna, M. Adamik, U. Kaiser, S. Laux, H. Bangert, M. Pulliainen, and K. A. Pischow, Surf. Coat. Technol. **100**, 72–75 (1998).

[28]P. Allongue, C. Henry de Villeneuve, S. Morin, R. Boukherroub, and D. D. M. Wayner, Electrochim. Acta **45**, 4591 (2000).

[29]I. Levine, S. M. Weber, Y. Feldman, T. Bendikov, H. Cohen, D. Cahen, and A. Vilan, Langmuir **28**, 404–415 (2012).

[30]C. W. Hollars and R. C. Dunn, Rev. Sci. Instrum. **69**, 1747 (1998).

[31]P. B. Barna and M. Adamik, Thin Solid Films **317**, 27–33 (1998).

[32]C. Eisenmenger-Sittner, J. Appl. Phys. **89**, 6085–6091 (2001).

[33]R. Stumpf and M. Scheffler, Phys. Rev. Lett. **72**, 254 (1994).

[34]K. Reichelt, Vacuum **38**, 1083–1099 (1988).

[35]Z. J. Liu, Y. G. Shen, L. P. He, and T. Fu, Appl. Surf. Sci. **226**, 371–377 (2004).

[36]H. Haick and D. Cahen, Acc. Chem. Res. **41**, 359–366 (2008).

[37]I. V. Markov, *Crystal Growth for Beginners*, 2nd ed. (World Scientific, Singapore, 2003).

[38]A. L. del Vecchio and F. Spaepen, J. Appl. Phys. **101**, 063518 (2007).

[39]L. Cui-Lian and H. Chin-Kun, Appl. Phys. Lett. **96**, 093101 (2010).

[40]B. W. Sloope and C. O. Tiller, J. Appl. Phys. **36**, 3174–3181 (1965).

[41]A.-L. Barabási and H. E. Stanley, *Fractal Concepts in Surface Growth* (Cambridge University Press, Great Britain, 1995).

[42]J. G. Amar, F. Family, and P.-M. Lam, Phys. Rev. B **50**, 8781–8797 (1994).

[43]M. J. Verkerk and G. J. van der Kolk, J. Vac. Sci. Technol. A **4**, 3101–3105 (1986).

[44]S. M. Binz, M. Hupalo, and M. C. Tringides, Phys. Rev. B **78**, 193407 (2008).

[45]See supplementary material at http://dx.doi.org/10.1063/1.4730411 for (1) different correlations of roughness with evaporation rate and thickness; (2) correlation of the data of Ref. 15 with Eqs. (2) and (3); (3) computation of estimated heating during UFTD; (4) residual gas analysis of evaporator chamber; (5) XPS survey scan of Al film; (6) AFM image of Al film deposited from an alternative boat made of Al_2O_3-coated W.